# 1 The Synergy of Low-NaOH Activation and Carbon Sequestration in Sustainable Red Mud

# 2 Based Geopolymer

- 3 Vinitha Mariyappan<sup>1</sup> and Karthiyaini Somasundaram<sup>2\*</sup>
- 4 Research Associate, School of Civil Engineering, Vellore Institute of Technology, Chennai -
- 5 600127, India
- <sup>2</sup> Professor, School of Civil Engineering, Vellore Institute of Technology, Chennai 600127,
- 7 India

10

11

12

13

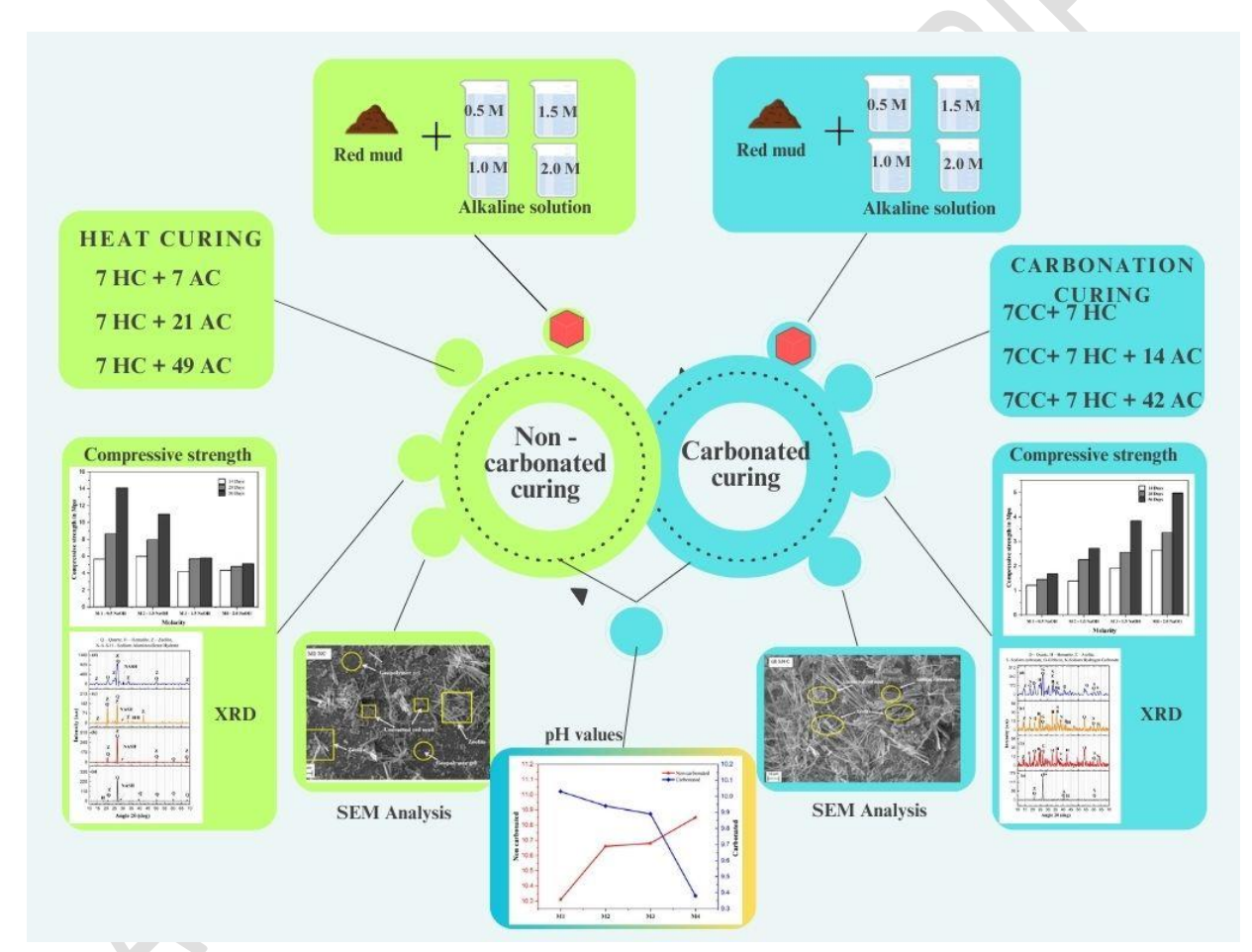
14

15

16

8 \*Corresponding author's e-mail: karthiyaini.s@vit.ac.in

# 9 Graphical Abstract:



### 1 ABSTRACT

- This research explores using low molarity sodium hydroxide (NaOH) in alkali activated red mud 2 based geopolymer mortars to enhance sustainability. Carbonation curing was employed to 3 capture CO<sub>2</sub> and promote mineral carbonation. The study assessed how NaOH molarity (0.5M 4 to 2M) affects physical, mechanical, microstructural properties and statistical analysis through 5 compressive strength, pH, crystalline characterization, microstructural analysis before and after 6 carbonation and ANOVA analysis. Non-carbonated samples showed highest compressive 7 strength at 0.5M NaOH, while carbonated samples peaked at 2M. Red mud's natural alkalinity 8 9 enhanced strength at low NaOH concentrations in non-carbonated conditions. Carbonated 10 samples showed greater strength at 2M due to higher Na<sup>+</sup> availability. XRD analysis identified geopolymer reaction products and unreacted phases in non-carbonated samples, while 11 carbonated ones showed sodium carbonate. SEM showed dense N-A-S-H gel at 0.5M in non-12 carbonated samples and zeolite needle formations and sodium carbonate crystals in carbonated 13 samples at 2M. pH increased with higher NaOH concentrations in non-carbonated samples and 14 decreased after carbonation. ANOVA revealed curing period affects compressive strength of red 15 mud geopolymer mortar, with M1-M3 gaining strength while M4 stabilized early. Results 16 indicate red mud's alkalinity enables effective geopolymerization at lower NaOH concentrations, 17 while higher NaOH concentration enhances CO<sub>2</sub> sequestration through carbonation curing, 18 highlighting potential for sustainable applications. 19
- Key words: Red mud, Carbonation curing, Sodium hydroxide (NaOH) molarity, Sustainable
   binder, Geopolymer mortar

### 1. Introduction

22

23

24

25

26

27

28

29

30

31

32

Concrete is essential to the construction sector and it is considered the most used building material due to its comparatively low cost, strength and raw material in mass production(Venkatesh & Shanmugasundaram, 2024). Globally, the output of ordinary Portland cement (OPC) continues to increase at a rate of 9% per annum. The significant amount of CO<sub>2</sub> released into the atmosphere during cement production makes this increase extremely dangerous to the environment(Nie et al., 2016). In particular, the annual emissions of greenhouse gases from the production of OPCs amount to approximately 2.3 billion tons, or 1.4 m<sup>3</sup> per person, on average (Liu, Liu & Zhang, 2024a).

Ordinary Portland Cement (OPC) is produced at extremely high temperatures, often between 900°C and 1500 °C, owing to the energy-intensive clinker formation process(Wei et al.,

2025). This leads to considerable CO<sub>2</sub> emissions. In contrast, geopolymerisation involves the interaction of aluminosilicate precursors (such as fly ash or slag) with alkaline solutions at significantly lower temperatures. This makes geopolymer production far more energy-efficient and environmentally friendly, providing a sustainable alternative to OPC by lowering energy usage and carbon emissions (Li et al., 2024). One ton of geopolymer cement produces only 0.184 tons of CO<sub>2</sub> emissions, making it nearly six times more environmentally friendly than one ton of regular Portland cement (OPC)(Sathsarani, Sampath & Ranathunga, 2023).

Geopolymer is a suitable replacement for regular concrete. Geopolymerization is the process of creating a polymeric network by mixing aluminosilicate rich in materials with an alkaline silicate solution. Research has already been done on varies industrial wastes, including fly ash(Suprakash, Karthiyaini & Shanmugasundaram, 2022), GGBS, Metakaolin(Chandralega, Shanmugasundaram & Stone, 2025), Copper slag, red mud/Bauxite Residue(Konduru & Karthiyaini, 2024), and Argo industry wastes. Alkali precursors are used in this method to produce a bonding agent that solidifies rapidly. When these connections are broken, as frequently happens in alkaline settings, geopolymers dissolve. In geopolymer materials with low CaO content, the predominant phase is a non-crystalline aluminosilicate gel called N-A-S-(H)(Han et al., 2023), which is made up of sodium oxide (Na<sub>2</sub>O), aluminium oxide (Al<sub>2</sub>O<sub>3</sub>), silicon dioxide (SiO<sub>2</sub>), and water (H<sub>2</sub>O). Among various industrial wastes explored for geopolymer production, bauxite residue (red mud) stands out due to its high iron oxide content and abundance as a byproduct of the aluminium industry and hence understanding its properties along with potential applications is crucial for sustainable material development.

Bauxite residue or red mud (RM) is a waste product of the aluminium industry(Li et al., 2020). Aluminium is the next often used metal after steel; however, due to its wide range of uses in modern society, it also generates a lot of waste(Simha, Yeddula & Somasundaram, 2020). In addition, this generation seriously endangers ecosystems. Annually, 150 million tons of red mud are generated, with less utilization which is leading to substantial environmental concerns(Liu et al., 2023). Additionally, 0.8–1.5 tonnes of bauxite residue are produced for every tonne of alumina produced(Evans, 2016). Bauxite residue is the primary precursor material employed in this investigation. Because it contains a high percentage of iron oxide, bauxite residue has a dark red colour(Duraisamy & Chaunsali, 2025). Due to its high alkalinity, red mud contaminates groundwater supplies and agricultural lands near its depository sites, posing a serious environmental threat. Red mud causes a risk to agricultural fields and groundwater airborne dust hazards, and potential catastrophic risks from storage dam failure.(Liu, Liu & Zhang, 2024a).During

carbonation, red mud's high pH levels can drop from 12 to 6.81(Mudgal et al., 2021), its alkalinity is reduced to lessen its negative effects on the environment and to make it safer to use as building material(Ilahi et al., 2024). The bonding behavior at the interface in Ni–nano-Al<sub>2</sub>O<sub>3</sub> coatings shows a similar reliance on processing conditions as seen in geopolymers made from red mud(Pradeep et al., 2021). Geopolymers made from a combination of 50% red mud and fly ash, activated using sodium hydroxide and sodium silicate, exhibit improved strength and reactivity. The process of mechanical activation and controlled curing enhances gel formation, resulting in a strength of approximately 27 MPa while effectively utilizing waste materials(Hao et al., 2025).

CO<sub>2</sub> is used in methanol production, urea creation, microalgae biofuel production, and fibre-based CO<sub>2</sub> reduction. Alkaline ions like calcium and magnesium react with CO<sub>2</sub> to generate stable carbonated molecules(Yang et al., 2024b). Compared to other CO<sub>2</sub> collection techniques, these carbon sequestration-derived compounds are more stable. To keep global temperatures below 2°C, mineral carbonation can result in negative emissions or significant CO<sub>2</sub> reductions(Chandralega, Shanmugasundaram & Stone, 2025). Research has focused on reducing CO<sub>2</sub> emissions by using mineral carbonation in construction materials. Carbonation process captures CO<sub>2</sub> and converts metal oxides into stable carbonate minerals, such as calcium(Zheng et al., 2025), sodium, magnesium, iron, and manganese carbonates(Lux et al., 2019). Industrial wastes like iron powder, red mud, and steel slag, rich in CaO and MgO(Liu et al., 2026), enable CO<sub>2</sub> sequestration through mineral carbonation, converting CO<sub>2</sub> into stable carbonates and transforming waste into valuable products(Sanna et al., 2014). Alkaline materials are projected to store 2.9 to 8.5 billion tons of CO<sub>2</sub> per annum by 2100, using indirect alkaline waste application and direct CO<sub>2</sub> mineralization(Liu, Liu & Zhang, 2024a). This could reduce CO<sub>2</sub> emissions, with possible annual decreases of up to 4.02 gigatons(Zhang et al., 2024b).

Geopolymer concrete (GPC), will also be significantly impacted by CO<sub>2</sub>, which will cause "carbonation" or a decrease in alkalinity from the exterior to the interior(Zhao et al., 2024). In geopolymer-based concrete systems, CO<sub>2</sub> and alkali ions in the pore solution(Bernal, 2015) react to form various carbonate hydrates, influenced by temperature(Lamaa et al., 2023), humidity(Cyr & Pouhet, 2016), and CO<sub>2</sub> concentration(Zhang et al., 2024a). The primary phases that develop during carbonation are anhydrous sodium carbonates (Na<sub>2</sub>CO<sub>3</sub>)(Cai, Pan & Yang, 2023), natron (Na<sub>2</sub>CO<sub>3</sub>·10H<sub>2</sub>O)(Bernal et al., 2013), nahcolite (NaHCO<sub>3</sub>)(Yamazaki et al., 2021), trona (Na<sub>3</sub>H(CO<sub>3</sub>)<sub>2</sub>·2H<sub>2</sub>O) and thermonatrite (Na<sub>2</sub>CO<sub>3</sub>·H<sub>2</sub>O)(Bernal et al., 2014). The carbonation reaction is driven from mass transfer, dissolution and reaction with ions. In Mass

Transfer, CO<sub>2</sub> moves from the environment into air-filled pores of the mortar(Harirchi & Yang, 2022). In Dissolution phases, CO<sub>2</sub> dissolves in pore solutions, forming bicarbonate (HCO<sup>3-</sup>) and carbonate ions (CO<sub>3</sub> <sup>2-</sup>)(Bernal et al., 2012a). Reaction with ion phases, dissolved group react with calcium, sodium, and magnesium to form carbonate precipitates, which reduces hydroxide ion concentration and lower its pH(Chandralega, Shanmugasundaram & Stone, 2025).

The replacement of 50% red mud with GGBS paste showed notable strength even at a low molarity of 2 M sodium hydroxide, and the compressive strength of the geopolymer mortar was further enhanced by lowering the sodium silicate-to-sodium hydroxide ratio from 2.5 to 1.5 (Singh, Aswath & S, 2024). Carbonation is enhanced by formation of Na<sub>2</sub>CO<sub>3</sub> and CaCO<sub>3</sub>, it improves permeability, lowers the void ratio by fine-tuning the pore structure, and increases microstructural stability and durability by combining with N-A-S-H gel to produce a hybrid system (Beltrame et al., 2023). Carbonation reduces pore volume and maximizes pore sizes in concrete in 1–4 days. This alteration results in a three to fivefold increase in fracture energies, thereby enhancing the material's ability to resist cracking(Das et al., 2014). CO<sub>2</sub> curing for 6 days promotes greater formation of carbonated phases within the concrete matrix, contributing to improved material properties and it enhances the strength(Saranya, Karthiyaini & Stone, 2025).

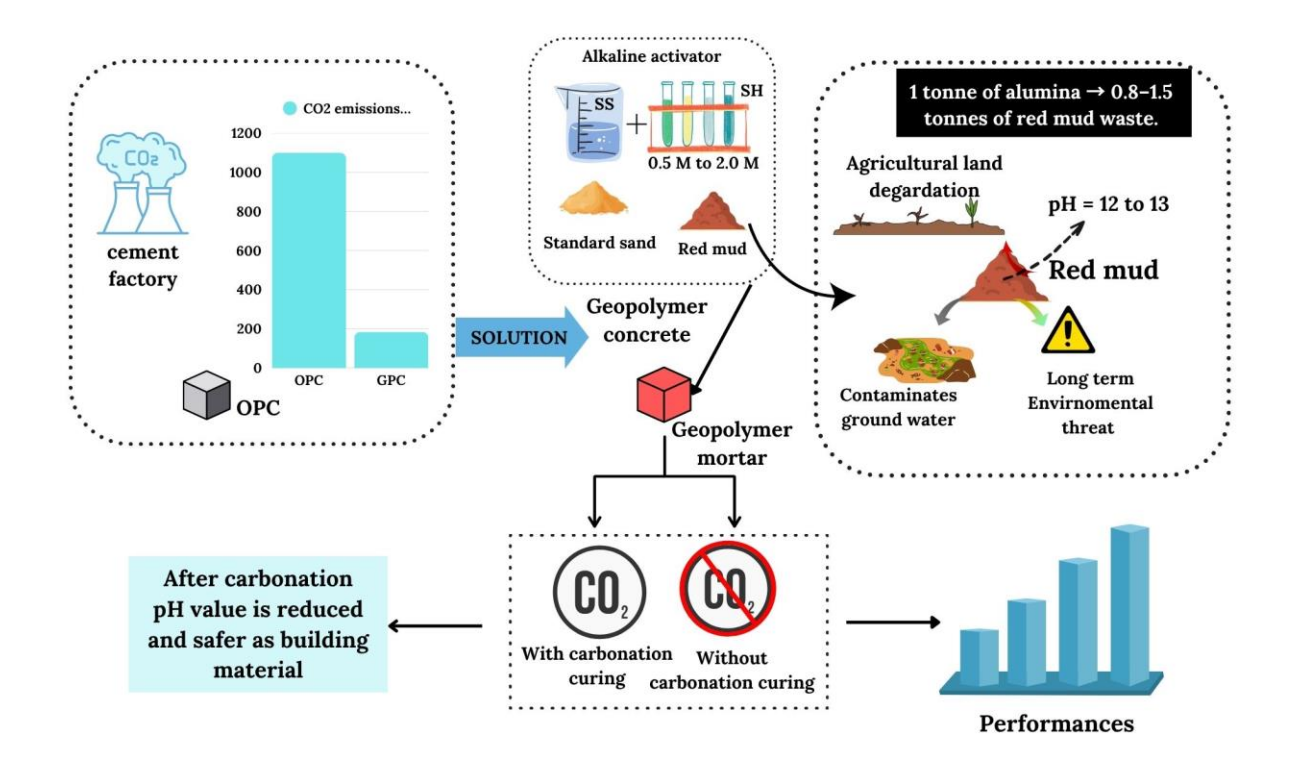


Figure 1. Workflow

A few studies have been conducted on carbonation curing in 100% red mud-based geopolymer mortars with lower molarities. The combined effects of alkali concentration and CO<sub>2</sub> exposure on the geopolymerization of red mud have not been investigated before. This study is unique in its examination of creating geopolymer mortar entirely from red mud, activated systematically with varying lower concentrations of NaOH and subjected to carbonation curing. And the study is also aimed to reduce NaOH usage and evaluate how its molarity (from 0.5M to 2M) influences the mortar's physical, mechanical, and microstructural characteristics was illustrated in Figure 1. Assessments included compressive strength, pH level, Microstructural analysis before and after carbonation curing and ANOVA analysis was done. Specifically, we sought to determine the optimal molarity for maximizing these properties, thereby contributing to the development of more durable and environmentally friendly building materials.

#### 2. Materials And Methods

#### 2.1. Materials

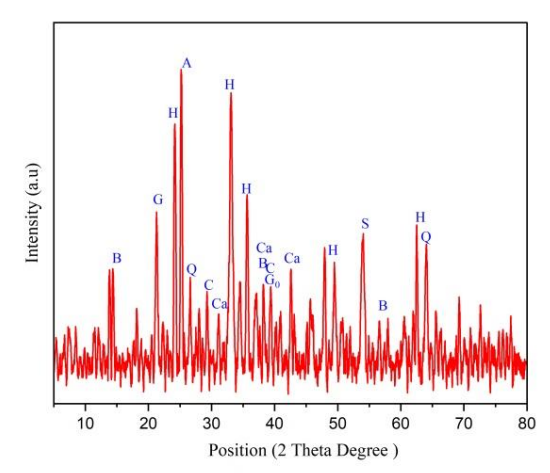
The raw materials utilized in this research comprise red mud, standard sand, Alkali activators (sodium hydroxide and sodium silicate) and water.

### 2.1.1. Red Mud

The red mud obtained from refining of aluminium production. Direct usage of the raw bauxite waste was hampered by a 6.85% loss of ignition due to the moisture content(Provis, Palomo & Shi, 2015). As a result, it was dried for 24 hours at 105°C in an oven. After this stage RM was allowed to settle in ambient temperature. The left-over RM was then crushed into a powder and passed to a 90-micron size to be utilized in the manufacture of the geopolymer mortar. It was dried, crushed and sieved in 90-micron sieve before testing(Lu et al., 2024). The chemical composition of untreated red mud was obtained from XRF (elemental analysis), and its mineralogical structure was analysed through XRD (crystalline phase identification) as shown in Table 1 and Figure 2. The chemical composition components of red mud are presented in Table 1.

# **Table 1.** Chemical composition of untreated red mud

Material	Chemical compositions (wt.%)								
Red Mud	Fe <sub>2</sub> O <sub>3</sub>	Al <sub>2</sub> O <sub>3</sub>	SiO <sub>2</sub>	TiO <sub>2</sub>	CaO	MgO	P <sub>2</sub> O <sub>5</sub>	SO <sub>3</sub>	K <sub>2</sub> O
	36.5	30.62	18.05	4.5	1.5	0.86	0.5	0.3	0.2



H-Hematite G-Geothite G<sub>0</sub> - Gibbsite Q- Quartz Ca- Cancrinite C-Calcite S- Sodalite

B-Bochmite A-Anatase

Figure 2. XRD of Raw red mud

### 2.1.2. Standard sand

The fine aggregate used in this study is Standard sand in compliance with IS 650:1991; three equal-proportion grades, grade I (1 mm to 2 mm), grade II (0.5 mm to 1 mm), grade III (0.09 mm to 0.5 mm) are combined in a planetary mixer until proper mixing is achieved as per standard and this sand is used for manufacturing of mortar cubes.

# 2.1.3. Alkaline Activator

Sodium hydroxide (NaOH) pellets with 99% purity are mixed with water till its complete dissolution for preparing NaOH solutions at different molarities (0.5M, 1M, 1.5M, and 2M). A solution of sodium silicate (Na<sub>2</sub>SiO<sub>3</sub>) with 33% soluble silicates is added with a freshly prepared NaOH solution to formulate an alkaline media; the NaOH solution must cool before being combined with the Na<sub>2</sub>SiO<sub>3</sub> solution, which should be made 24 hours before specimens are cast.

#### 2.2. Methods

### 2.2.1. Preparation of Sodium Hydroxide Solution and alkaline solution

A Liter of distilled water was mixed with sodium hydroxide flakes the day before casting to create the sodium hydroxide solution. Subsequent laboratory measurements determined the molarity. A specified amount of sodium hydroxide (NaOH) solids is dissolved in one liter of distilled water. The solution is then gently stirred and allowed to cool to room temperature before adding the sodium silicate solution(Zakira et al., 2023; Bernal et al., 2012b). For example, to prepare 2 molarity of NaOH, weight of 80g of NaOH pellets dissolved in one litre of deionized water and make up to total volume.

# 2.2.2. Mix proportions

The proportion of materials was taken from ASTM 109C/C109M-20a as 1 parts of binder: 2.75 parts of standard sand for standard mortar and the mix proportion of this study is discussed in table. The red mud is used as 100% binder with standard sand. The molarity of NaOH solution is varied from 0.5 to 2 M with 0.5 M interval. And liquid to binder ratio(L/B) is fixed as 0.5 throughout the study and sodium silicate and sodium hydroxide ratio fixed as 2 as shown in Table 2.

**Table 2.** Mix proportions are given in kg/cm<sup>3</sup>

Mix ID	Description	Red mud (kg)	Standard sand(kg)	NaOH solids (kg/cm³)	Water (L)	SS (kg/cm <sup>3</sup>	Total liquid(L)	L/B ratio	NaOH molarity
M1 NC		X		0.20	1				0.5 M
M2 NC	Non -			0.40	1				1 M
M3 NC	Carbonated			0.60	1				1.5 M
M4 NC		1.48	4.07	0.80	1	2	3	0.5	2 M
M1 C		1.40	4.07	0.20	1	2	3	0.3	0.5 M
M2 C	Carbonated			0.40	1				1 M
М3 С	Carbonated			0.60	1				1.5 M
M4 C				0.80	1				2 M

2.2.3. Sample preparation, curing condition, experimental methods and statistical analysis

Figure 3 shows the preparation of red mud-based geopolymer mortar, curing conditions and experimental methods. Initially, the red mud is oven-dried and then sieved through a 90-micron sieve, to be used as the primary precursor. The standard sand is added as per standard.

Next, the sieved red mud and standard sand are dry mixed thoroughly in a mixer. After proper dry mixing, the required quantity of alkaline activator is added, and wet mixing is done.

According to ASTM C109/C109M-20a, the mortar is poured into 50 mm x 50 mm x 50 mm moulds. The mortar is filled in two layers, with each layer properly compacted. One set of samples in the moulds is immediately placed in carbonation curing for 7 days, while another set is kept for heat curing after demoulding. In this study two curing conditions are adopted. First, oven curing condition for HC + AC (7 Heat curing + Ambient curing) ( $27^{\circ} \pm 2C$ , Relative humidity (RH) of  $60 \pm 10\%$ ) and samples were cured for 14 days, 28 days and 56 days. Second, carbonation curing condition for 7 CC + 7 HC + AC (Carbonation curing + Heat curing + Ambient curing) and samples were cured for 14 days, 28 days and 56 days. The carbonation curing was kept at  $30 \pm 2$  °C and  $85 \pm 5\%$  relative humidity. To maintain saturation, CO<sub>2</sub> gas was periodically replenished at a rate of 50 kg/cm<sup>2</sup>. To evaluate the effectiveness of the binder under CO<sub>2</sub> exposure, samples were cured for 7 days. Totally 3 specimens were casted for each curing and molarity including 14, 28 & 56 days.

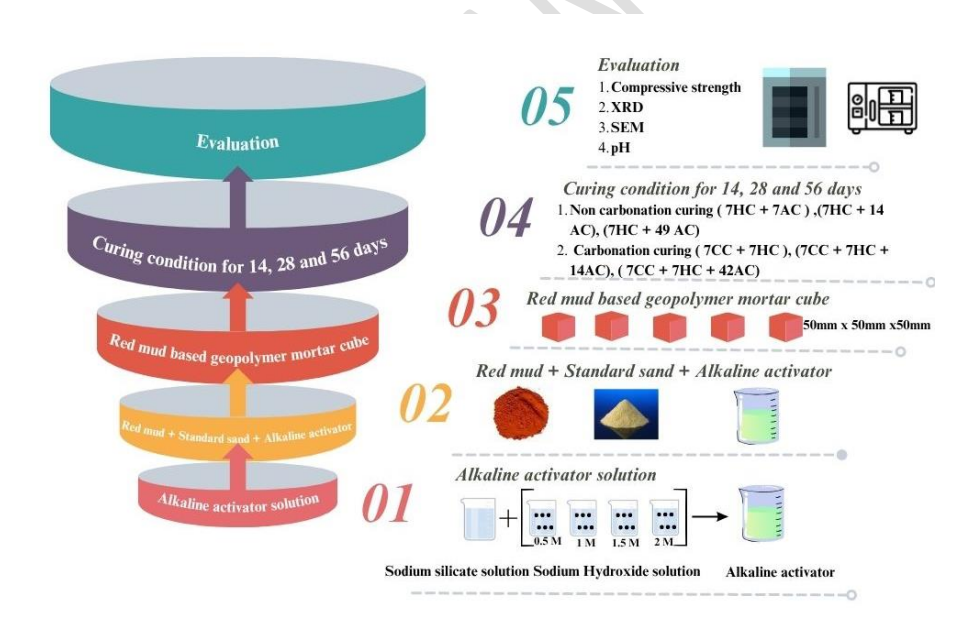


Figure 3. Sample preparation, curing condition and experimental methods

The compression testing machine with a maximum load capacity of 2000 kN was utilized to carry out the standardized testing procedures. Cube specimens 50 mm on each side were subjected to a continuous load of 0.15 MPa/s until collapse occurred. In compliance with ASTM C109, the compressive strength tests were conducted. Three specimens were evaluated to ascertain the compressive strength for each mixture. The mineralogical analysis of red mud was

executed using XRD RIGAKU Smartlab 3kW apparatus Powder X-Ray Diffraction, with an 1 interval of 0.02° with scanning speed of 5° per minute, with Cu - Kα radiation, a scan range of 2 3 5-80° 20 and graphs were plotted using origin pro software. The mortar samples were subjected to microstructural examination using a CARL ZEISS scanning electron microscope (SEM). 4 5 Specimens that were carbonated and those that were conventionally cured were inspected at different magnifications (500x to 5000x). The pH is measured using pH metre. The specimens 6 are crushed and ground by the solid-liquid extraction process before being passed through a 7 conventional sieve with a 75-micron pore size. When the dry powder is combined with deionized 8 9 water at a ratio of 1:10 (i.e. 3g of dry powder with 30 ml of deionized water). The sample is sealed and stir for the period of 8hours, the resultant mixture can be analysed(Han et al., 2023). 10 11 The surface of the specimens was taken from 0-10mm depth for carbonated samples and noncarbonated samples using diamond cutting to ensure undisturbed sample. The relevance of 12 various parameters on compressive strength was assessed using the analysis of variance 13 (ANOVA). When determining whether each element will have a substantial impact on the 14 indicator (i.e., the compressive strength), ANOVA may adjust for the error and variation of the 15 test findings. The factor has a stronger effect on the indication when the value of p is smaller and 16 the number of F is higher(ZHANG et al., 2023). 17

### 3. Results And Discussion

3.1. Compressive Strength

18

19

22

23

24

25

26

27

28

29

30

31

32

33

3.1.1. Impact of Sodium Hydroxide Concentration on Non-Carbonated Geopolymer
 Mortar's Compressive Strength

Figure 4 shows that the compressive strength of non-carbonated red mud mortar cubes containing various concentrations of sodium hydroxide was evaluated at different curing periods: 14 days (7HC + 7AC), 28 days (7HC + 21AC), and 56 days (7HC + 49AC). The graph illustrates the relationship between compressive strength (MPa) and curing time (days). The M1 NC demonstrated a notable strength increase on 28 days with 52.65% in comparison to 14 days, followed by an additional 62.98% increase on 56 days in comparison to 28 days. This suggests that the M1 NC mixture continues to gain strength beyond 28 days, proving most effective in the long term due to extended ambient curing conditions(Singh Assistant Professor & Aswath Professor, 2017). The M2 NC also showed considerable strength gains, with increases on 28 days with 33.16% in comparison to 28 days and 38.30% increase in comparison to 28 to 56 days, although not as substantial as M1 NC. The M3 NC exhibited only a minor strength increase of 1.93% between 28 to 56 days, indicating an early strength attainment. The M4 NC have a lesser

strength compared with all the mixes, and the strength increases on 28 days with 12.60% on comparison to 14 days. Also increase in strength of 45.87% between 28 and 56 days in compression.

M1 NC has 43.61% of strength gain compared to M2 NC and 74.00% strength gain than M3 NC. The M1 NC has 122.78% strength gain than M4 NC. Red mud's inherent alkalinity eliminates the need for high molar alkaline activators. At M1 NC, the solution likely enhances the dissolution of aluminosilicate materials, promoting the formation of Geopolymer matrix bonds over time(Chindawong et al., 2025). The excessive alkalinity in M2 NC, M3 NC and M4 NC may impede the dissolution process and delay geopolymerization gel formation(Singh, Aswath & S, 2024). Increased molarity impedes the leaching of aluminium and silicate ions, thereby slowing the geopolymerization process. Furthermore, a higher concentration of OH<sup>-</sup> ions results in the premature precipitation of aluminosilicate gel, which consequently hinders geopolymerization.

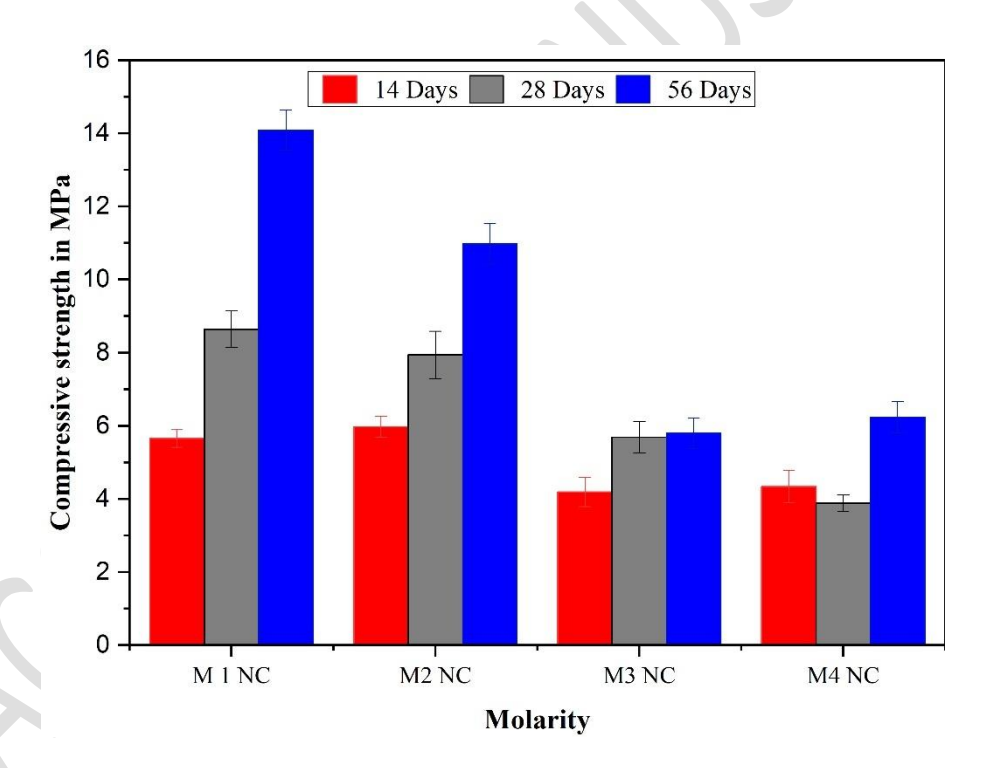


Figure 4. Compressive Strength of Geopolymer Mortar without carbonation

3.1.2. Impact of Sodium Hydroxide Concentration on the Compressive Strength of Carbonated Geopolymer Mortar

The compressive strength of red mud based geopolymer mortar with increasing sodium hydroxide molarity of 0.5M to 2M and carbonation curing is shown in the Figure 5. While cement

hydration involves the reaction of calcium hydroxide with CO<sub>2</sub> to form calcium carbonate, the geopolymerization process in red mud-based mortars follows a different mechanism(Ilahi et al., 2024). But when it comes to geopolymer mortar, the combination of red mud precursor and alkali activators like NaOH and Na<sub>2</sub>SiO<sub>3</sub> (Shi et al., 2024), were converted into a three-dimensional network structure composed of [AlO<sub>4</sub>]<sup>5-</sup> and [SiO<sub>4</sub>]<sup>4-</sup> tetrahedral units through the processes of dissolution, diffusion, and repolymerization(Yan et al., 2024). The presence of Na<sup>+</sup> played a crucial role in influencing the structure of the geopolymer matrix (Bao et al., 2020).

In M1 C sodium hydroxide concentration as reduced strength attainment. From 14 days to 56 days increased by 42%. The limited amount of sodium ions leads to forms alkali activation for red mud based geopolymer mortar. If sodium ions are not participated in the formation of matrix. However, the sodium ions were captured by CO<sub>2</sub> to form a sodium carbonate crystal(Xiaoshuang et al., 2024). The formation of crystals to induce the internal stress on the geopolymer mortar weaken bonds, poor structure, more porosity and it affects compressive strength(Shi et al., 2024).

In contract at M2 C, the compressive strength improves as compared with 0.5M, by 93%. The compressive strength is continuously increased for 14 to 56 days on 1.5M, by 100%. The compressive strength was observed to be highest at a concentration of 2M. As the NaOH concentrations increase to 1M to 2M, there is a notable increase in the availability of sodium ions compared to the concentration of 0.5M. When free alkali is present, especially at higher NaOH concentrations, it increases the sodium ion content in the alkaline activator(Nie et al., 2016). During the carbonation process, these sodium ions creating bond with CO<sub>2</sub> (Yang et al., 2024b), forming sodium carbonate crystals(Longhi et al., 2020). This interaction leads to the obstruction of pores within the geopolymer matrix, resulting in denser structure with decreased porosity(Li et al., 2024). Consequently, this densification process enhances the strength of the geopolymer mortar in higher molarity(Beltrame et al., 2023).

The findings indicate a pattern of enhanced compressive strength as sodium hydroxide concentrations increase from 0.5M to 2M. This enhancement is linked to intensified geopolymerization and generation of sodium carbonate crystals, resulting in a more compact structure with reduced porosity. The study underscores the importance of optimizing alkali activator concentrations in achieving enhanced mechanical characteristics in geopolymer mortars. These insights are valuable for developing sustainable construction materials utilizing industrial by-products(Liu et al., 2024b) such as red mud.

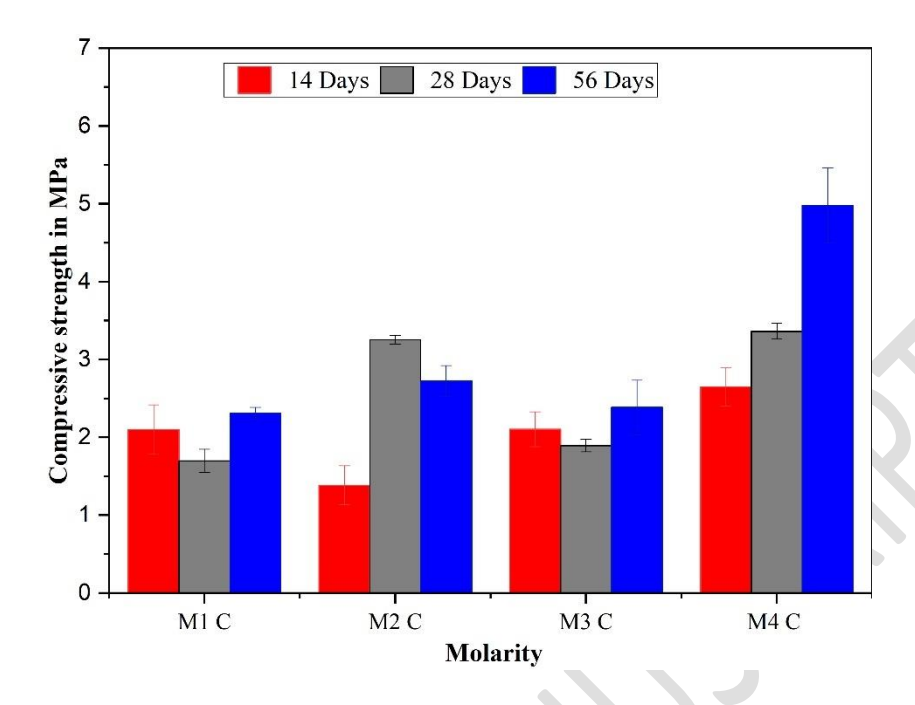


Figure 5. Compressive Strength of Geopolymer Mortar with carbonation

# 3.2. Appearance of carbonated red mud Geopolymer mortar

The formation of efflorescence on surface of carbonated samples is due to chemical reaction between the alkalis in the geopolymer activator and presences of carbon di oxide(Werling et al., 2020). Efflorescence formation depends on temperature, humidity and mainly due to availability of Na<sup>+</sup> and OH<sup>-</sup> which is present in alkali activation. The mechanisms of white deposit on surface of samples are reaction of excess alkali oxides present in the pore structure of geopolymer samples with CO<sub>2</sub> which diffuses the geopolymer matrix(Shi et al., 2024). It evaporates from its surface, which results in alkali rich cation on the pore solution and forming white sodium carbonate deposits on the surface(Liu et al., 2024a).

The Figure 6 shows that the images of carbonated sample and microstructure analysis of white efflorescence on the surface of carbonated samples. The XRD shows the formation of sodium carbonate and small amount of sodium bi carbonate phases. SEM- EDS gives the evidence for sodium carbonate on the efflorescence.

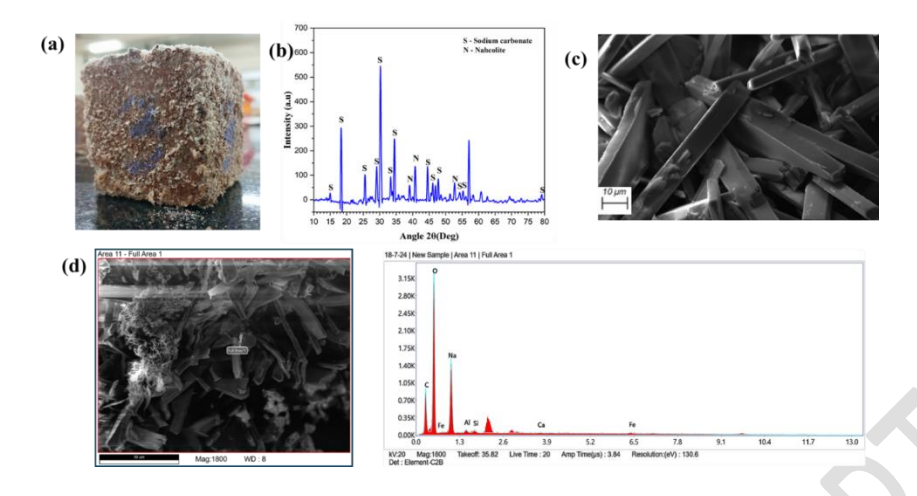


Figure 6. Appearance of carbonated samples

# 3.3. X-Ray Diffraction Analysis

1

2

3

4

5

6

7

8

9

10

11

12

13

14

15

16

17

18

19

20

21

22

23

# 3.3.1. XRD analysis for non-carbonated red mud based geopolymer mortar

X-ray diffraction (XRD) analysis was conducted to investigate the phase composition of non-carbonated red mud-based geopolymer mortar samples M1 NC, M2 NC, M3 NC, and M4 NC after 56 days, as illustrated in Figure 7. All samples exhibited the presence of quartz (SiO<sub>2</sub>)(Jiang et al., 2024), with its most prominent peak observed at approximately 26.0°, consistent with previous research(Yang et al., 2024a). Quartz functions as a filler in the geopolymer, contributing to its structural formation(Nie et al., 2016). The development of N-A-S-H (sodium aluminosilicate hydrate) gel was observed in all samples between 20.0°-40.0°. This characteristic of gel in low-calcium precursors, is essential for enhancing the strength (Bajpai, Shrivastava & Singh, 2020) and durability of the geopolymer matrix (Bernal et al., 2010). In M1 NC, the N-A-S-H gel remained in an amorphous state, forming a compact and denser structure (Ai et al., 2021), along with quartz. In contrast, in M2 NC, M3 NC and M4 NC, the N-A-S-H gel coincided with zeolite phases. This overlap hindered the dissolution of silica and alumina from aluminosilicate precursors, resulting in a delayed formation of the geopolymer matrix (Chen et al., 2019). Hematite was identified in all samples, indicating the presence of some unreacted red mud(Sufian Badar et al., 2014). The M1 NC sample contained the lowest amount of unreacted hematite, while the other samples M2 NC, M3 NC, and M4 NC exhibited higher hematite content. The emergence of crystalline zeolite phases in M2 NC, M3 NC, and M4 NC led to increased porosity and microcracking within these samples. These crystalline phases induced internal stresses, causing a decrease in compressive strength(Shi et al., 2024).

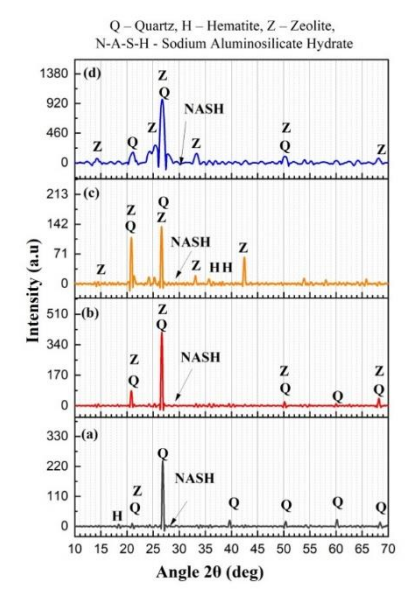


**Figure 7.** XRD analysis of non-carbonated samples (a) M1 NC, (b) M2 NC, (c) M3 NC and (d) M4 NC

# 3.3.2. XRD analysis for carbonated red mud based geopolymer mortar

1

2

3

4

5

6

7

8

9

10

11

12

13

14

15

16

17

18

19

20

21

22

Figure 8 displays X-ray diffraction (XRD) patterns revealing the phase composition of red mud-based geopolymer mortar subjected to carbonation curing with NaOH concentrations ranging from 0.5M to 2M. The primary crystalline phases identified through XRD analysis include Quartz (Q), Hematite (H), Zeolite (Z), Sodium carbonate (S), Gibbsite (G), and Sodium hydrogen carbonate (N). In M1 C, quartz, hematite, and gibbsite phases were prominent, with minor contributions from sodium carbonate and zeolite phases, suggesting limited geopolymerization due to low NaOH concentration. Quartz peaks were observed at 26.0°,40.0° and 60.0° indicating the stability of red mud-based geopolymer mortar as a primary source in red mud(Singh, Aswath & S, 2024). Hematite peaks were noted along 33.0° in all mixes except M1 C. The presence of gibbsite in M1 C mix indicates incomplete dissolution of precursors(Shi et al., 2020). In M2 C higher intensity peaks for zeolite and sodium carbonate compared to M1C, matrix and carbonation due enhancing geopolymer to increased concentration(Ozcelikci et al., 2023). Zeolite phase peaks around 20.0° and 15.0° represent secondary geopolymerization reactions, leading to structural densification and improved strength compared to M1 C (Ai et al., 2021). Sodium carbonate crystalline peaks were identified at 18.0°,38.0°,29.0° and 59.0° alongside quartz, reflecting the reaction between CO<sub>2</sub> and sodium ions in the alkali activator during carbonation(Xue et al., 2018). This process results in a denser, more compact structure with enhanced strength due to pore filling. The M3 C mix showed strong

zeolite peaks along with quartz, sodium carbonate, and some sodium hydrogen carbonate peaks, the latter being a byproduct of the carbonation process. M4 C displayed even stronger peaks of sodium carbonate and zeolite compared to M3 C, attributed to the higher NaOH concentration of 2M. This reflects the combined effect of increased NaOH concentration and the carbonation process. Among the 0.5M, 1M, and 1.5M mixes, M4 C demonstrated the highest compressive strength.

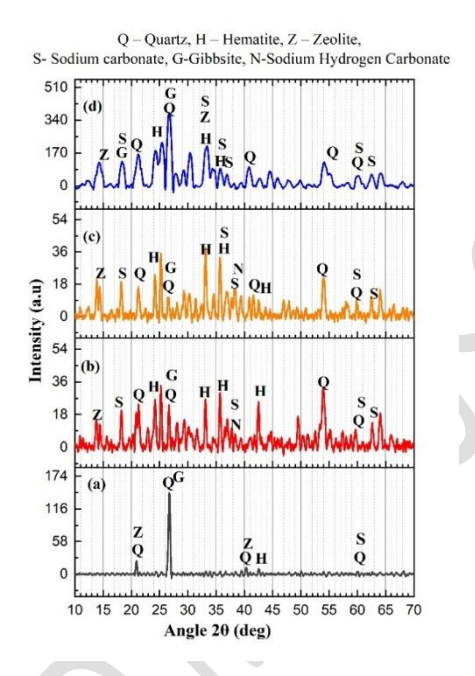


Figure 8. XRD analysis of carbonated samples (a) M1 C, (b) M2 C, (c) M3 C and (d) M4 C

3.4. Scanning Electron Microscope Analysis

3.4.1. SEM analysis for non-carbonated red mud based geopolymer mortar

Figure 9 shows the SEM images of samples M1 NC, M2 NC, M3 NC and M4 NC at 56 days at 5000x magnification. In M1 NC looks like a dense structure, invisible cracks and compared to that of M2 NC, M3 NC and M4 NC samples. N-A-S-H gel was fully formed, and limited unreacted red mud is seen, indicating that fully reacted structure. In M1 NC, small amount of needle like crystal is present. M1 NC has the maximum compressive strength because of N-A-S-H gel formation. The M2 NC sample displayed varied solidified phases that had come together to form distinct clusters of particles. Each unit body had a loose arrangement, fissures, and comparatively high porosity. Geopolymer gels were found in sheets and clusters, as seen in Figure 9. The gels were cross connected to create a continuous pore. A comparison with Figure 9 reveals that more needle-like particles formed from unreacted red mud particles whose surface was coated in a tiny bit of geopolymer gel. In references with XRD Figure 7, Zeolite phases were

- 1 overlapped with N-A-S-H gel and the reactivity of geopolymer matrix is reduced. According to
- 2 this, too much alkalinity might delay the dissolution process, the geopolymerization reaction was
- 3 not complete, and some material remained unreacted (Liu et al., 2020).

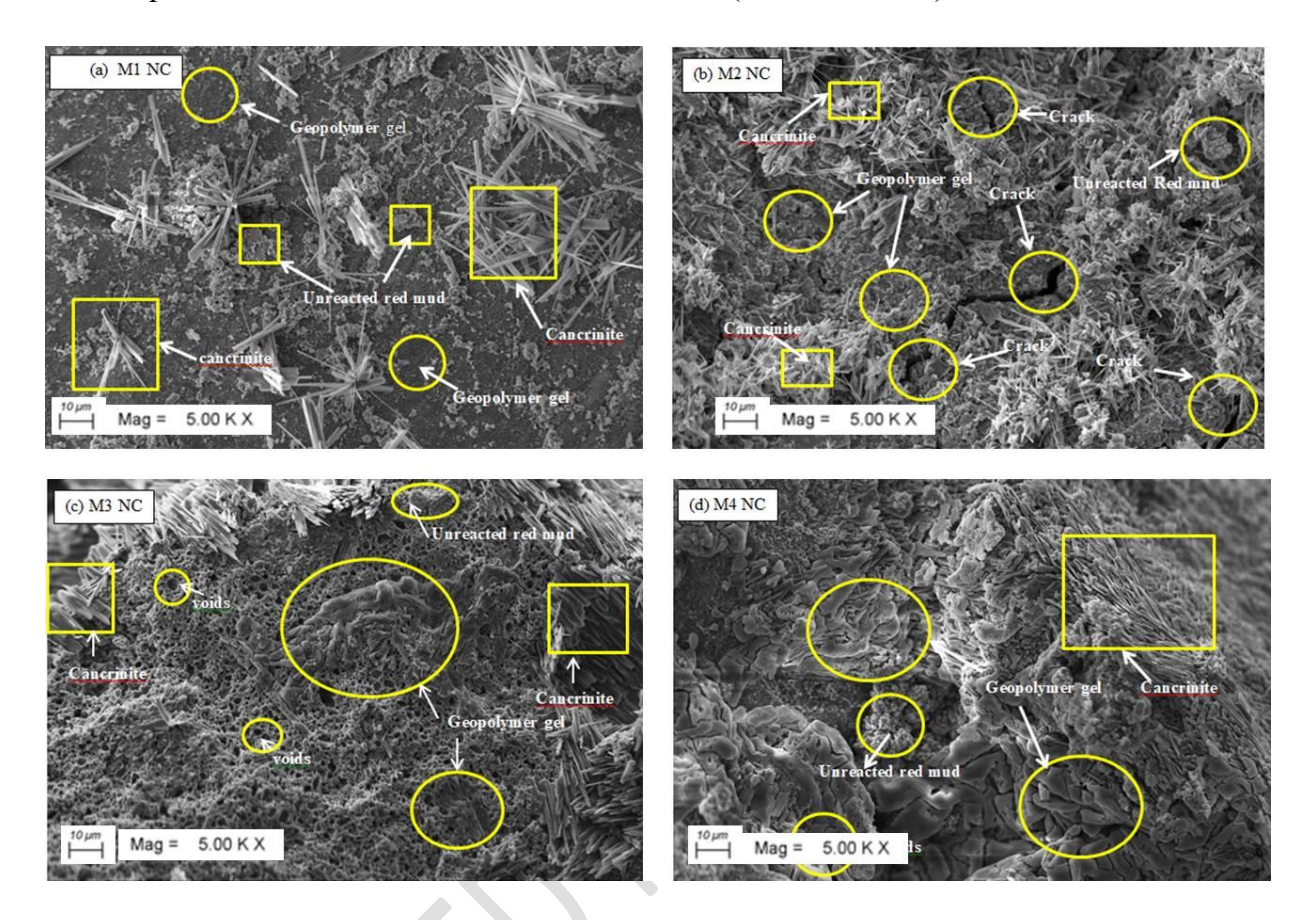


**Figure 9.** SEM images of non-carbonated red mud geopolymer mortar (a) M1 NC, (b) M2 NC, (c) M3 NC and (d) M4 NC

The surface becomes non uniform, as seen in Figure 9, and the Geopolymer gels were comparatively uneven. The dense structure had voids and was not complete, which reduced the compactness as compared to M1 C. This is why the M2 NC, M3 NC and M4 NC has less compressive strength as compared with M1 NC.

# 3.4.2. SEM analysis for carbonated red mud based geopolymer mortar

Red mud-based geopolymer mortar at carbonation curing with different NaOH concentrations M1 C, M2 C, M3 C, and M4 C is shown in Figure 10. Disintegrated structure, with unreacted red mud particles are visible in the geopolymer at M1 C. The low amount of sodium carbonate and zeolite crystals presence suggests that there are not enough geopolymerization gels because of the lower NaOH concentration(Mahfoud et al., 2024). A better reaction having uniform distribution and may improve needle-like production of sodium

carbonate and zeolite crystals were achieved by raising the concentration of NaOH to 1M (M2 C). Nevertheless, M2 C exhibits partial geopolymerization with some visible gaps and unreacted red mud particles. At M3 C, the microstructure is more structured with zeolite crystals and sodium carbonate, as well as some voids. Red mud dissolves more readily at this concentration, although some red mud particles remain unreacted and have not completely reacted. The compact structure is finally achieved at M4 C. Densely packed zeolite crystals with sodium carbonate show a higher degree of geopolymerization after carbonation curing. Overall, the findings show that silica and alumina from red mud dissolves more readily when the molarity of NaOH is increases, which improves matrix polymerization and densification.

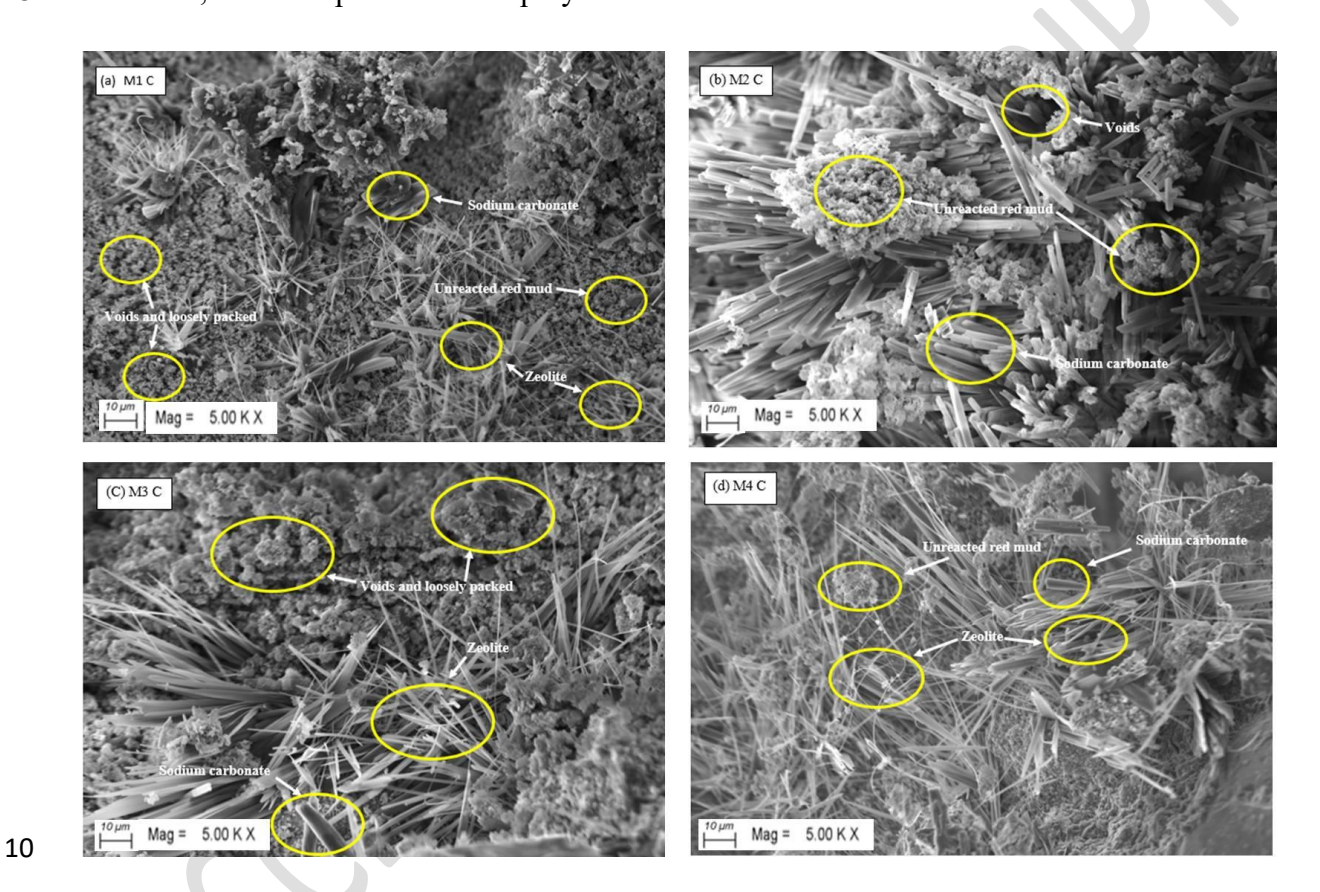


**Figure 10.** Sem images of carbonated red mud based Geopolymer mortar (a) M1 C, (b) M2 C, (c) M3 C & (d) M4 C

The best results are obtained at 2M NaOH, where the carbonation curing process promotes a cohesive microstructure with few voids and unreacted elements, making it appropriate for greater durability and mechanical strength.

## 3.5. pH on carbonated and non- carbonated red mud based geopolymer mortar

Figure 11 illustrates the pH levels of red mud-based geopolymer mortar at various NaOH concentrations under both non-carbonated and carbonated curing conditions. For non-

carbonation, pH increases as NaOH concentration rises. It commences at 10.3 for M1 NC, and increases significantly to 10.7 at M2 NC, further it remains relatively constant between M2 NC and M3 NC. A subsequent increase is observed at M4 NC (10.8). Sodium ions (Na<sup>+</sup>) are essential in maintaining high pH levels in the pore solution, which is critical for geopolymerization(Han et al., 2023). Red mud and alkali activators function as the primary sources of Na<sup>+</sup> ions(Liu, Liu & Zhang, 2024b). As NaOH concentration increases, a greater quantity of Na<sup>+</sup> ions remain in the pore solution even after N-A-S-H gel formation(Yamazaki et al., 2021).

Conversely, carbonated samples exhibit an inverse trend, with pH decreasing steadily as NaOH concentration rises. The pH initially is at 11.0 for M1 C, and marginally decreases to 10.9 at M2 C, further it remains constant at M3 C. There is a sharp decrease to 9.4 at M4 C. Generally, higher molar alkali activator accelerates carbonation rates in geopolymer concrete(Nguyen et al., 2022). Prior to carbonation, excess Na<sup>+</sup> in the pore solution contributes to maintaining high pH. However, when excess Na<sup>+</sup> interacts with CO<sub>2</sub>, it produces sodium carbonate and sodium bicarbonate, resulting in further pH reduction (Yamazaki et al., 2021). These observations emphasize the impact of carbonation, which significantly reduces alkalinity by forming carbonate and bicarbonate compounds, particularly at higher NaOH concentrations(Zhao et al., 2024).

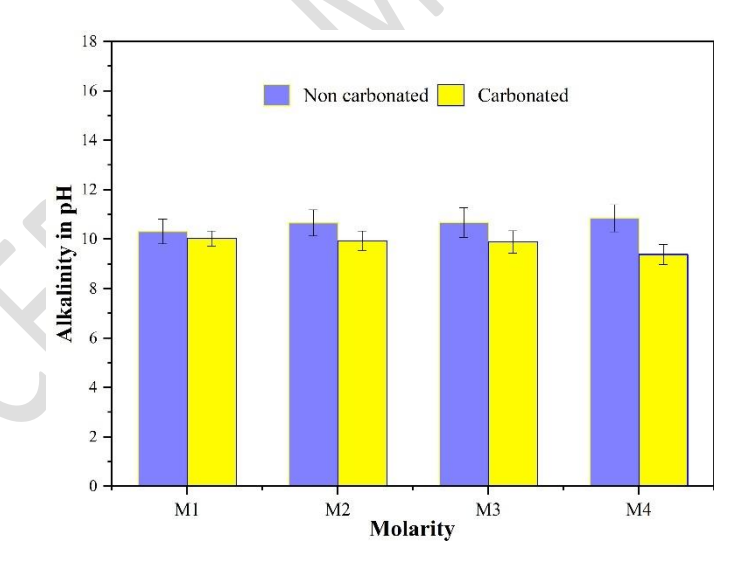


Figure 11. pH on carbonated and non-carbonated samples

3.6. ANOVA analysis of compressive strength for both non-carbonated & carbonated samples

# 1 Table 3. ANOVA results of compressive strength both carbonated and non-carbonated red mud

### 2 based geopolymer mortar

Mix ID	P- values							
	14 DAYS	28 DAYS	56 DAYS					
M 1	4.20232E-07	1.48789E-07	1.04848E-09					
M 2	0.0002	0.002	0.003					
М 3	0.0013	7.41525E-06	0.0003					
M 4	0.172	0.042	0.259					

3

4

5

6 7

8

9

10

11

12

13

14

15

16

17

18

19

20

21

22

23

24

The ANOVA results of compressive strength of non-carbonated and carbonated samples of red mud based geopolymer mortar as shown in Table 3. The statistical hypothesis test indicates that a factor has a substantial impact on the response value if the p-value is less than 0.05, and vice versa(Yao et al., 2024). At 14 days, mixes M1, M2, and M3 had P-values < 0.05, showing a significant difference in curing times. This implies that the curing time has a significant impact on the early-age compressive strength of these mixes, mainly because of the fast dissolution of aluminosilicate species and later polycondensation that forms the initial geopolymeric gel network(He et al., 2024). M4, on the other hand, had a P-value of 0.172 and did not significantly change with curing time, so it might due to a slower rate of geopolymerization or a decreased availability of reactive phase in the early phases(Liu et al., 2023). At 28 days, M1, M2, and M3 showed substantial differences (P < 0.05), indicating gel formation and structural densification as curing progresses. M4's marginally significant P-value of 0.042 suggests that between days 14 and 28, there was some small structural rearrangement or subsequent gel formation. At 56 days, mixes M1-M3 still had very low P-values, indicating that these systems were undergoing microstructural refinement, probably due to the slow transition of amorphous aluminosilicate gels into more stable three-dimensional networks. After 28 days, however, M4's P-value of 0.259 indicated no statistically significant strength improvement. This implies that M4 has reduced ongoing geopolymerization despite achieving near-complete reaction and microstructural stability previously. Overall, the ANOVA results demonstrate that the curing duration has a substantial effect on the compressive strength of mixes M1-M3, although M4 exhibits reasonably steady performance following early cure.

### 4. Conclusions

- 2 This study investigates the feasibility of producing red mud-based geopolymer mortar using low-
- 3 concentration alkaline solutions, while considering both carbonated and non-carbonated curing
- 4 conditions. The investigation analysed compressive strength, Microstructural analysis and pH
- 5 levels leading to the following findings:
  - 1. Lower NaOH concentration (0.5M) resulted in higher long-term compressive strength in non-carbonated red mud-based geopolymer mortar. M1 NC (0.5M NaOH) exhibited the most significant strength gains over time, indicating that moderate alkalinity optimally promotes aluminosilicate dissolution and gradual geopolymer matrix formation.
    - 2. Higher NaOH concentrations (1M, 1.5M, and 2M) led to reduced strength gains in non-carbonated samples due to excessive alkalinity hindering ion leaching and causing early precipitation of aluminosilicate gel, slowing geopolymerization. This suggests that red mud's inherent alkalinity is sufficient to reduce the need for high concentrated alkaline activators.
    - 3. In carbonated red mud-based geopolymer mortar, increasing NaOH concentration (0.5M 2M) enhanced strength by improving geopolymerization and reducing porosity. Higher NaOH concentrations (1M 2 M) facilitated N-A-S-H matrix formation, with maximum strength achieved at 2M, highlighting the role of alkali in optimizing sustainable cement alternatives.
    - 4. XRD analysis of non-carbonated samples confirmed quartz as a filler and N-A-S-H gel formation in all samples, essential for strength. M1 NC exhibited a dense structure with amorphous N-A-S-H gel, while M2 NC, M3 NC, and M4 NC contained overlapping zeolite phases, hindering geopolymerization. Higher hematite content in these samples indicated more unreacted red mud. The presence of crystalline zeolite phases increases the porosity and microcracking, reducing compressive strength.
    - 5. Conversely, XRD analysis of carbonated samples showed that increasing NaOH concentration enhanced geopolymerization and densification. Lower NaOH (0.5M) led to incomplete dissolution, while higher concentrations (1M–2M) promoted zeolite and sodium carbonate formation, improving strength. The strongest peaks at 2M indicated optimal properties, highlighting alkali concentration's role in sustainable geopolymer development.
    - 6. SEM analysis of non-carbonated samples showed that the low NaOH concentration (0.5M) produced a dense structure with fully formed N-A-S-H gel, leading to the highest

- strength. In contrast, higher concentrations (1M, 1.5M, and 2M) resulted in cracks, higher porosity, and unreacted red mud, reducing compactness and strength due to excessive alkalinity hindering geopolymerization.
  - 7. SEM analysis of carbonated samples indicated that increasing NaOH concentration may improve the geopolymerization and densification. At M1 C, presence of voids and unreacted particles led to poor packing. At M2 C, sodium carbonate and zeolite crystals formed, even though gaps persist. At M3 C, the structure improves with better red mud dissolution. The most compact matrix appeared at M4 C, with densely packed crystals, confirming the role of NaOH in enhancing microstructure and strength.
  - 8. Non-carbonated red mud-based geopolymer maintained high pH levels with increasing NaOH concentration due to excess sodium ions (Na<sup>+</sup>) in the pore solution, supporting geopolymerization process.
    - 9. In contrast, carbonated samples exhibited a gradual pH decrease as Na<sup>+</sup> ions reacted with CO<sub>2</sub>, forming sodium carbonate and bicarbonate, leading to reduced alkalinity. This suggests that higher NaOH concentrations expedite carbonation, potentially improves long-term durability.
    - 10. The ANOVA results clearly show that the development of compressive strength in red mud-based geopolymer mortar is considerably impacted by curing period. At every curing age, mixes M1, M2, and M3 showed statistically significant differences (P < 0.05), demonstrating that prolonged curing encourages gel formation, microstructural densification, and geopolymerization.
    - 11. On the other hand, M4 did not exhibit any notable fluctuation after 28 days, indicating that its geopolymeric reactions were mostly finished earlier, producing a stable matrix with little further strength gain.

# **Future Scope**

- 27 Red mud-based geopolymers present significant potential for developing low-carbon
- 28 construction materials and enhancing CO<sub>2</sub> sequestration through optimized carbonation
- techniques.

• Evaluate long-term durability and mechanical performance of carbonated and noncarbonated red mud-based geopolymers under aggressive environmental conditions and aging.

- Study the combined use of sodium silicate or other alkali sources with low molarity
   NaOH to balance strength and cost.
- Conduct a detailed life cycle assessment (LCA) to compare environmental impacts with OPC and other geopolymers, including quantification of CO<sub>2</sub> uptake and net carbon savings.

# **Competing Interest**

6

7

8

9

13

19

The authors declare that they have no known competing financial interests or personal relationships that could have appeared to influence the work reported in this paper.

# **CRediT** authorship contribution statement

- 10 Vinitha M.: Writing original draft, Visualization, Validation, Methodology,
- 11 Investigation, Conceptualization. S Karthiyaini: Writing review & editing, Supervision,
- 12 Methodology, Conceptualization.

# Acknowledgment

- The authors express their gratitude to the Vellore Institute of Technology, Chennai, for
- the necessary support in implementing this work. Additionally, we would like to express our
- deep gratitude to Dr. M. Shanmugasundaram, Associate Professor, School of Civil Engineering,
- 17 Vellore Institute of Technology, Chennai, for his valuable insights that significantly aided in the
- 18 completion of this study.

# Data availability

Data will be made available on request.

### 21 REFERENCE

- 22 Ai, T., Zhong, D., Zhang, Y., Zong, J., Yan, X. & Niu, Y. (2021) The effect of red mud content on the
- compressive strength of geopolymers under different curing systems. Buildings. 11 (7).
- 24 doi:10.3390/buildings11070298.
- Bajpai, R., Shrivastava, A. & Singh, M. (2020) Properties of fly ash geopolymer modified with red mud
- and silica fume: a comparative study. SN Applied Sciences. 2 (11). doi:10.1007/s42452-020-03665-3.
- Bao, J., Li, S., Zhang, P., Xue, S., Cui, Y. & Zhao, T. (2020) Influence of exposure environments and
- 28 moisture content on water repellency of surface impregnation of cement-based materials. *Journal of*
- 29 *Materials Research and Technology*. 9 (6), 12115–12125. doi:10.1016/j.jmrt.2020.08.046.

- Beltrame, N.A.M., Dias, R.L., Witzke, F.B. & Medeiros-Junior, R.A. (2023) Effect of carbonation 1
- curing on the physical, mechanical, and microstructural properties of metakaolin-based geopolymer 2
- 3 concrete. Construction and Building Materials. 406. doi:10.1016/j.conbuildmat.2023.133403.
- 4 Bernal, S.A. (2015) The resistance of alkali-activated cement-based binders to carbonation. In:
- 5 Handbook of Alkali-Activated Cements, Mortars and Concretes. Elsevier Inc. pp. 319–332.
- 6 doi:10.1533/9781782422884.3.319.
- 7 Bernal, S.A., de Gutierrez, R.M., Provis, J.L. & Rose, V. (2010) Effect of silicate modulus and
- metakaolin incorporation on the carbonation of alkali silicate-activated slags. Cement and Concrete 8
- 9 Research. 40 (6), 898–907. doi:10.1016/j.cemconres.2010.02.003.
- 10 Bernal, S.A., Provis, J.L., Brice, D.G., Kilcullen, A., Duxson, P. & Van Deventer, J.S.J. (2012a)
- Accelerated carbonation testing of alkali-activated binders significance, and role of pore solution chemistry. *Cement and Concrete Research*. 42 (10), 1317–1326. Accelerated carbonation testing of alkali-activated binders significantly underestimates service life: The 11
- 12
- 13
- 14 Bernal, S.A., Provis, J.L., Brice, D.G., Kilcullen, A., Duxson, P. & Van Deventer, J.S.J. (2012b)
- Accelerated carbonation testing of alkali-activated binders significantly underestimates service life: The 15
- role of pore solution chemistry. Cement and Concrete Research. 42 (10), 1317–1326. 16
- doi:10.1016/j.cemconres.2012.07.002. 17
- 18 Bernal, S.A., Provis, J.L., Walkley, B., San Nicolas, R., Gehman, J.D., Brice, D.G., Kilcullen, A.R.,
- 19 Duxson, P. & Van Deventer, J.S.J. (2013) Gel nanostructure in alkali-activated binders based on slag
- 20 and fly ash, and effects of accelerated carbonation. Cement and Concrete Research. 53, 127-144.
- 21 doi:10.1016/j.cemconres.2013.06.007.
- Bernal, S.A., San Nicolas, R., Myers, R.J., Mejía De Gutiérrez, R., Puertas, F., Van Deventer, J.S.J. & 22
- 23 Provis, J.L. (2014) MgO content of slag controls phase evolution and structural changes induced by
- 24 accelerated carbonation in alkali-activated binders. Cement and Concrete Research. 57, 33-43.
- 25 doi:10.1016/j.cemconres.2013.12.003.
- Cai, T., Pan, R. & Yang, M. (2023) Study on the effect of structural sodium dissolution on the physical 26
- 27 properties of red mud treated by sulfuric acid. Minerals Engineering. 204.
- 28 doi:10.1016/j.mineng.2023.108424.
- 29 Chandralega, V., Shanmugasundaram, M. & Stone, D. (2025) Enhancing the performance of iron-based
- binders with seawater and CO2 sequestration. Case Studies in Construction Materials. 22. 30
- 31 doi:10.1016/j.cscm.2025.e04367.
- 32 Chen, X., Guo, Y., Ding, S., Zhang, H., Xia, F., Wang, J. & Zhou, M. (2019) Utilization of red mud in
- 33 geopolymer-based pervious concrete with function of adsorption of heavy metal ions. Journal of
- 34 Cleaner Production. 207, 789–800. doi:10.1016/j.jclepro.2018.09.263.
- 35 Chindawong, C., Mekrattanachai, P., Pimraksa, K. & Setthaya, N. (2025) Strength optimization of
- 36 geopolymer pastes synthesized from high calcium bottom ash and red clay: A study of composition and
- 37 activation parameters. Advances in Science and Technology Research Journal. 19 (3), 299–308.
- 38 doi:10.12913/22998624/199987.
- 39 Cyr, M. & Pouhet, R. (2016) Carbonation in the pore solution of metakaolin-based geopolymer. Cement
- 40 and Concrete Research. 88, 227–235. doi:10.1016/j.cemconres.2016.05.008.

- Das, S., Stone, D., Convey, D. & Neithalath, N. (2014) Pore- and micro-structural characterization of a
- 2 novel structural binder based on iron carbonation. *Materials Characterization*. 98, 168–179.
- 3 doi:10.1016/j.matchar.2014.10.025.
- 4 Duraisamy, S. & Chaunsali, P. (2025) Stabilization of red mud using mineral carbonation. Cleaner
- 5 *Engineering and Technology*. 25. doi:10.1016/j.clet.2025.100926.
- 6 Evans, K. (2016) The History, Challenges, and New Developments in the Management and Use of
- 7 Bauxite Residue. *Journal of Sustainable Metallurgy*. 2 (4), 316–331. doi:10.1007/s40831-016-0060-x.
- 8 Han, W., Lv, Y., Wang, S., Qiao, J., Zou, C., Su, M. & Peng, H. (2023) Effects of Al/Na and Si/Na
- 9 Molar Ratios on the Alkalinity of Metakaolin-Based Geopolymer Pore Solutions. *Materials*. 16 (5).
- 10 doi:10.3390/ma16051929.
- Hao, H., Liu, X., Dong, X., Li, J., Li, J., Xu, X. & Chang, S. (2025) Study on the optimal ratios and
- strength formation mechanism of mechanical activation red mud based geopolymer. Journal of Building
- 13 Engineering. 104. doi:10.1016/j.jobe.2025.112401.
- Harirchi, P. & Yang, M. (2022) Exploration of Carbon Dioxide Curing of Low Reactive Alkali-
- 15 Activated Fly Ash. *Materials*. 15 (9). doi:10.3390/ma15093357.
- He, J., Guo, T., Li, Z., Gao, Y. & Zhang, J. (2024) Hydration mechanism of red mud-fly ash based
- geopolymer. *Materials Chemistry and Physics*. 314. doi:10.1016/j.matchemphys.2023.128807.
- 18 Ilahi, K., Debbarma, S., Mathew, G. & Inyang, H.I. (2024) Carbon capture and mineralisation using red
- mud: A systematic review of its principles and applications. *Journal of Cleaner Production*.473.
- 20 doi:10.1016/j.jclepro.2024.143458.
- 21 Jiang, Z., He, G., Jiang, Y., Zhao, H., Duan, Y., Yuan, G. & Fu, H. (2024) Synergistic preparation and
- properties of ceramic foams from wolframite tailings and high-borosilicate waste glass. *Construction*
- 23 *and Building Materials*. 457. doi:10.1016/j.conbuildmat.2024.139367.
- Konduru, H. & Karthiyaini, S. (2024) Enhancing solidification in one-part geopolymer systems through
- 25 alkali-thermal activation of bauxite residue and silica fume integration. Case Studies in Construction
- 26 *Materials*. 21. doi:10.1016/j.cscm.2024.e03444.
- Lamaa, G., Duarte, A.P.C., Silva, R.V. & de Brito, J. (2023) Carbonation of Alkali-Activated Materials:
- 28 A Review. Materials.16 (8). doi:10.3390/ma16083086.
- 29 Li, B., Wu, H., Liu, X., Zhu, T., Liu, F. & Zhao, X. (2020) Simultaneous removal of SO2 and NO using
- a novel method with red mud as absorbent combined with O3 oxidation. Journal of Hazardous
- 31 *Materials*. 392. doi:10.1016/j.jhazmat.2020.122270.
- Li, J., Liu, X., Cai, C., Li, F., Jin, H., Zhang, S., Sheng, N., Wang, T. & Ngo, T. (2024) Microstructure,
- 33 strength development mechanism and CO2 emission assessments of molybdenum tailings collaborative
- 34 fly ash geopolymers. Case Studies in Construction Materials. 21. doi:10.1016/j.cscm.2024.e03608.
- Liu, J., Lu, Y., Bai, X., Han, P., Xie, R. & He, B. (2020) Strength Characteristics and Electrochemical
- 36 Impedance Spectroscopy Characterization of Red Mud-Coal Metakaolin Geopolymers. *International*
- *Journal of Electrochemical Science*. 15 (11), 10694–10706. doi:10.20964/2020.11.03.

- 1 Liu, J., Ren, Y., Li, Z., Niu, R., Xie, G., Zhang, W. & Xing, F. (2024a) Efflorescence and mitigation of
- 2 red mud–fly ash–phosphogypsum multicomponent geopolymer. Construction and Building Materials.
- 3 448. doi:10.1016/j.conbuildmat.2024.137869.
- 4 Liu, M., Liu, H., Zhu, P., Chen, C., Wang, X. & Xu, L. (2024b) Recycling potential evaluation of
- 5 geopolymer concrete with different cementitious system used in freeze-thaw environment. Case Studies
- 6 *in Construction Materials*. 21. doi:10.1016/j.cscm.2024.e03535.
- 7 Liu, X., Liu, X. & Zhang, Z. (2024a) Application of red mud in carbon capture, utilization and storage
- 8 (CCUS) technology. Renewable and Sustainable Energy Reviews.202. doi:10.1016/j.rser.2024.114683.
- 9 Liu, X., Liu, X. & Zhang, Z. (2024b) Application of red mud in carbon capture, utilization and storage
- 10 (CCUS) technology. Renewable and Sustainable Energy Reviews.202. doi:10.1016/j.rser.2024.114683.
- Liu, Y., Han, Y., Shi, T., Lv, B., Zhang, F. & Zhou, X. (2026) An innovative method for preparing nano
- steel slag powder and analysis of carbonation reaction mechanism toward enhanced CO2 sequestration.
- 13 *Materials Letters*. 403. doi:10.1016/j.matlet.2025.139411.
- Liu, Y., Zhuge, Y., Chen, X., Duan, W., Fan, R., Outhred, L. & Wang, L. (2023) Micro-
- chemomechanical properties of red mud binder and its effect on concrete. *Composites Part B:*
- 16 Engineering. 258, 110688. doi:10.1016/j.compositesb.2023.110688.
- Longhi, M.A., Rodríguez, E.D., Walkley, B., Zhang, Z. & Kirchheim, A.P. (2020) Metakaolin-based
- 18 geopolymers: Relation between formulation, physicochemical properties and efflorescence formation.
- Composites Part B: Engineering. 182. doi:10.1016/j.compositesb.2019.107671.
- 20 Lu, J., Shen, Y., Wang, Y., Zhang, H., Guan, X., Zhu, J. & Liu, S. (2024) In-situ wet carbonation
- 21 activation of red mud waste for sustainable grout materials. Journal of Industrial and Engineering
- 22 *Chemistry*. 136, 453–464. doi:10.1016/j.jiec.2024.02.034.
- Lux, S., Baldauf-Sommerbauer, G., Ottitsch, B., Loder, A. & Siebenhofer, M. (2019) Iron Carbonate
- 24 Beneficiation Through Reductive Calcination Parameter Optimization to Maximize Methane
- 25 Formation. European Journal of Inorganic Chemistry. 2019 (13), 1748–1758.
- doi:10.1002/ejic.201801394.
- 27 Mahfoud, E., Ndiaye, K., Maherzi, W., Aggoun, S., Abriak, N.E. & Benzerzour, M. (2024) Carbonation
- 28 in just add water geopolymer based on fly ash and dredged sediments mix. Construction and Building
- 29 *Materials*. 452. doi:10.1016/j.conbuildmat.2024.138959.
- 30 Mudgal, M., Singh, A., Chouhan, R.K., Acharya, A. & Srivastava, A.K. (2021) Fly ash red mud
- 31 geopolymer with improved mechanical strength. Cleaner Engineering and Technology. 4.
- 32 doi:10.1016/j.clet.2021.100215.
- Nguyen, T.N., Phung, Q.T., Yu, Z., Frederickx, L., Jacques, D., Sakellariou, D., Dauzeres, A., Elsen, J.
- & Pontikes, Y. (2022) Alteration in molecular structure of alkali activated slag with various water to
- binder ratios under accelerated carbonation. Scientific Reports. 12 (1). doi:10.1038/s41598-022-09491-
- 36 4.
- Nie, Q., Hu, W., Ai, T., Huang, B., Shu, X. & He, Q. (2016) Strength properties of geopolymers derived
- 38 from original and desulfurized red mud cured at ambient temperature. Construction and Building
- 39 *Materials*. 125, 905–911. doi:10.1016/j.conbuildmat.2016.08.144.

- 1 Ozcelikci, E., Kul, A., Gunal, M.F., Ozel, B.F., Yildirim, G., Ashour, A. & Sahmaran, M. (2023) A
- 2 comprehensive study on the compressive strength, durability-related parameters and microstructure of
- 3 geopolymer mortars based on mixed construction and demolition waste. *Journal of Cleaner Production*.
- 4 396. doi:10.1016/j.jclepro.2023.136522.
- 5 Pradeep, D.G., Sharath, B.N., Afzal, A., Ahmed Ali Baig, M. & Shanmugasundaram, M. (2021) Study
- 6 on scratch behavior of Ni-Al2O3 coating composition on Al-2219 substrate by electro deposited
- 7 technique. *Materials Today: Proceedings*. 46, 8716–8722. doi:10.1016/j.matpr.2021.04.033.
- 8 Provis, J.L., Palomo, A. & Shi, C. (2015) Advances in understanding alkali-activated materials. *Cement*
- 9 *and Concrete Research*.78 pp.110–125. doi:10.1016/j.cemconres.2015.04.013.
- Sanna, A., Uibu, M., Caramanna, G., Kuusik, R. & Maroto-Valer, M.M. (2014) A review of mineral
- carbonation technologies to sequester CO2. *Chemical Society Reviews*.43 (23) pp.8049–8080.
- doi:10.1039/c4cs00035h.
- 13 Saranya, V., Karthiyaini, S. & Stone, D. (2025) Enhancement of strength and microstructural
- characterization in red mud-iron carbonate binders: Effects of CO2 sequestration and oxalic acid
- concentration. *Results in Engineering*. 25. doi:10.1016/j.rineng.2025.104539.
- Sathsarani, H.B.S., Sampath, K.H.S.M. & Ranathunga, A.S. (2023) Utilization of fly ash-based
- 17 geopolymer for well cement during CO2 sequestration: A comprehensive review and a meta-analysis.
- 18 *Gas Science and Engineering*.113. doi:10.1016/j.jgsce.2023.204974.
- 19 Shi, X., Lyu, S., Wang, Q., Xiao, J. & Li, Y. (2024) Experimental study on the effect of carbonate ions
- on ITZs of geopolymeric recycled concrete. Construction and Building Materials. 446.
- 21 doi:10.1016/j.conbuildmat.2024.137919.
- Shi, Y., Zhang, Z., Sang, Z. & Zhao, Q. (2020) Microstructure and Composition of Red Mud-Fly Ash-
- 23 Based Geopolymers Incorporating Carbide Slag. Frontiers in Materials. 7.
- 24 doi:10.3389/fmats.2020.563233.
- 25 Simha, B., Yeddula, R. & Somasundaram, K. (2020) Effect of red mud proportion on the strength and
- 26 microstructure of ferrosialate based geopolymer mortar. *Indian Journal of Engineering & Materials*
- 27 Sciences.27.
- 28 Singh Assistant Professor, S. & Aswath Professor, M.U. (2017) Effect of Curing Methods On The
- 29 Property of Red Mud Based Geopolymer Mortar. International Journal of Civil Engineering and
- 30 *Technology (IJCIET)*. 8 (10), 1481–1489.
- 31 http://www.iaeme.com/IJCIET/index.asp1481http://http://www.iaeme.com/ijciet/issues.asp?JType=IJCI
- 32 ET&VType=8&IType=10http://www.iaeme.com/IJCIET/issues.asp?JType=IJCIET&VType=8&IType
- 33 =10http://www.iaeme.com/IJCIET/index.asp1482.
- 34 Singh, S., Aswath, M.U. & S, T.B. (2024) Effect of silica on the properties of red mud based
- 35 geopolymer mortar for synthesis of sustainable bricks. *Journal of Building Pathology and*
- 36 Rehabilitation. 9 (1). doi:10.1007/s41024-024-00424-4.
- 37 Sufian Badar, M., Kupwade-Patil, K., Bernal, S.A., Provis, J.L. & Allouche, E.N. (2014) Corrosion of
- 38 steel bars induced by accelerated carbonation in low and high calcium fly ash geopolymer concretes.
- 39 Construction and Building Materials. 61, 79–89. doi:10.1016/j.conbuildmat.2014.03.015.

- 1 Suprakash, A.S., Karthiyaini, S. & Shanmugasundaram, M. (2022) A study on compressive strength of
- 2 ultrafine graded fly ash replaced concrete and machine learning approaches in its strength prediction.
- 3 Structural Concrete. 23 (6), 3849–3863. doi:10.1002/suco.202100778.
- 4 Venkatesh, V. & Shanmugasundaram, M. (2024) Enhancement of mechanical and microstructural
- 5 characteristics of magnesium oxychloride cement with metasteatite. Case Studies in Construction
- 6 *Materials*. 21. doi:10.1016/j.cscm.2024.e03683.
- Wei, M., Chen, L., Lei, N., Li, H. & Huang, L. (2025) Mechanical properties and microstructures of
- 8 thermally activated ultrafine recycled fine powder cementitious materials. Construction and Building
- 9 *Materials*. 475. doi:10.1016/j.conbuildmat.2025.141195.
- Werling, N., Dehn, F., Krause, F., Steudel, A., Schuhmann, R. & Emmerich, K. (2020) SOLUBILITY
- 11 OF PRECURSORS AND CARBONATION OF WATERGLASS-FREE GEOPOLYMERS. Clays and
- 12 Clay Minerals. 68 (5), 524–531. doi:10.1007/s42860-020-00096-4.
- 13 Xiaoshuang, S., Yanpeng, S., Jinqian, L., Yuhao, Z. & Ruihan, H. (2024) Preparation and performance
- optimization of fly ash- slag- red mud based geopolymer mortar: Simplex-centroid experimental design
- method. Construction and Building Materials. 450. doi:10.1016/j.conbuildmat.2024.138573.
- 16 Xue, X., Liu, Y.L., Dai, J.G., Poon, C.S., Zhang, W.D. & Zhang, P. (2018) Inhibiting efflorescence
- 17 formation on fly ash–based geopolymer via silane surface modification. Cement and Concrete
- 18 *Composites*. 94, 43–52. doi:10.1016/j.cemconcomp.2018.08.013.
- 19 Yamazaki, Y., Kim, J., Kadoya, K. & Hama, Y. (2021) Physical and chemical relationships in
- accelerated carbonation conditions of alkali-activated cement based on type of binder and alkali
- 21 activator. *Polymers*. 13 (4), 1–17. doi:10.3390/polym13040671.
- Yan, S., Wang, W., He, C., Gai, X. & Wang, S. (2024) Characterization and properties of porous red
- 23 mud-based geopolymer composites reinforced with carbon fiber powders. Diamond and Related
- 24 *Materials*. 111531. doi:10.1016/j.diamond.2024.111531.
- Yang, J., Wang, Z., Luo, H., Wang, H., Chen, L., Liu, M., Tang, M. & He, B.J. (2024a) Preparation and
- 26 properties of alkali-activated red mud-based artificial lightweight aggregates. Construction and
- 27 *Building Materials*. 449. doi:10.1016/j.conbuildmat.2024.138304.
- Yang, J., Xiao, H., He, X., Zeng, J., Su, Y., Li, W., Wang, Y. & Jin, Z. (2024b) Effect of wet grinding
- 29 carbonation of sintering red mud on the performance of carbon sequestered mortar. Construction and
- 30 *Building Materials*. 445. doi:10.1016/j.conbuildmat.2024.137933.
- 31 Yao, Z., Luo, L., Qin, Y., Cheng, J. & Qu, C. (2024) Research on mix design and mechanical
- 32 performances of MK-GGBFS based geopolymer pastes using central composite design method.
- 33 Scientific Reports. 14 (1). doi:10.1038/s41598-024-59872-0.
- Zakira, U., Zheng, K., Xie, N. & Birgisson, B. (2023) Development of high-strength geopolymers from
- red mud and blast furnace slag. *Journal of Cleaner Production*. 383. doi:10.1016/j.jclepro.2022.135439.
- 36 ZHANG, L., CHEN, Z., CHEN, R., ZHU, S., LIN, J. & TAI, P. (2023) Compressive strength of fly ash
- 37 based geopolymer utilizing waste completely decomposed granite. Case Studies in Construction
- 38 *Materials*. 19. doi:10.1016/j.cscm.2023.e02667.

- 1 Zhang, X., Wang, X., Zhan, Q. & Song, C. (2024a) Carbonation reaction properties and reaction
- 2 mechanisms of red mud under different carbon dioxide pressures. Journal of Environmental Chemical
- 3 Engineering. 12 (3). doi:10.1016/j.jece.2024.112910.
- 4 Zhang, Y., Zhan, G., Huang, Z., Xing, L., Ying, Y., Chen, Z. & Li, J. (2024b) Performance and
- 5 mechanisms of alkaline solid waste in CO2 mineralization and utilization. Waste Management. 175, 62–
- 6 72. doi:10.1016/j.wasman.2023.12.047.

13

14

15

16

17

18

- 7 Zhao, C., Li, Z., Peng, S., Liu, J., Wu, Q. & Xu, X. (2024) State-of-the-art review of geopolymer
- 8 concrete carbonation: From impact analysis to model establishment. Case Studies in Construction
- 9 *Materials*. 20. doi:10.1016/j.cscm.2024.e03124.
- 10 Zheng, M., Zhang, Y., Yan, S., Wu, Z., Li, X., Wu, D. & Xiong, L. (2025) Effect of carrier-
- encapsulated microbial calcium carbonate on the performance of cement mortar. Construction and
- 12 *Building Materials*. 483. doi:10.1016/j.conbuildmat.2025.141579.